

University of Texas Rio Grande Valley

**ScholarWorks @ UTRGV**

---

Physics and Astronomy Faculty Publications  
and Presentations

College of Sciences

---

7-24-2018

## Asymmetric Free-Space Light Transport at Nonlinear Metasurfaces

Nir Shitrit

Jeongmin Kim

David S. Barth

Hamidreza Ramezani

Yuan Wang

*See next page for additional authors*

Follow this and additional works at: [https://scholarworks.utrgv.edu/pa\\_fac](https://scholarworks.utrgv.edu/pa_fac)

 Part of the [Astrophysics and Astronomy Commons](#)

---

### Recommended Citation

Nir Shitrit, et. al., (2018) Asymmetric Free-Space Light Transport at Nonlinear Metasurfaces. Physical Review Letters 121:4. DOI: <http://doi.org/10.1103/PhysRevLett.121.046101>

This Article is brought to you for free and open access by the College of Sciences at ScholarWorks @ UTRGV. It has been accepted for inclusion in Physics and Astronomy Faculty Publications and Presentations by an authorized administrator of ScholarWorks @ UTRGV. For more information, please contact [justin.white@utrgv.edu](mailto:justin.white@utrgv.edu), [william.flores01@utrgv.edu](mailto:william.flores01@utrgv.edu).

---

**Authors**

Nir Shitrit, Jeongmin Kim, David S. Barth, Hamidreza Ramezani, Yuan Wang, and Xiang Zhang

# Asymmetric Free-Space Light Transport at Nonlinear Metasurfaces

Nir Shitrit<sup>1†</sup>, Jeongmin Kim<sup>1†</sup>, David S. Barth<sup>1</sup>, Hamidreza Ramezani<sup>1</sup>, Yuan Wang<sup>1</sup>, and Xiang Zhang<sup>1,2\*</sup>

<sup>1</sup>*NSF Nanoscale Science and Engineering Center (NSEC),  
3112 Etcheverry Hall, University of California, Berkeley, California 94720, USA*

<sup>2</sup>*Materials Sciences Division, Lawrence Berkeley National Laboratory,  
1 Cyclotron Road, Berkeley, California 94720, USA*

(Dated: May 29, 2018)

<sup>†</sup>These authors contributed equally to this work.

\*Corresponding author. E-mail: [xiang@berkeley.edu](mailto:xiang@berkeley.edu)

## Abstract

Asymmetric light transport has significantly contributed to fundamental science and revolutionized advanced technology in various aspects such as unidirectional photonic devices, optical diodes and isolators. While metasurfaces mold wavefronts at will with an ultrathin flat optical element, asymmetric transport of light cannot be fundamentally achieved by any linear system including linear metasurfaces. We report asymmetric transport of free-space light at nonlinear metasurfaces upon transmission and reflection. Moreover, we theoretically derived the nonlinear generalized Snell's laws that were experimentally confirmed by the anomalous nonlinear refraction and reflection. The asymmetric transport at optically thin nonlinear interfaces is revealed by the concept of reversed propagation path. Such an asymmetric transport at metasurfaces opens a new paradigm for free-space ultrathin lightweight optical devices with one-way operation including unrivaled optical valves and diodes.

Wave propagation, from sound to light, is generally two-way symmetric, i.e., forward and backward paths are identical. Nevertheless, the quest for protecting a laser from back reflections or improving information capacity in optical communication technology by mitigating a multipath interference calls for asymmetric transport (AT). AT is an uneven physical response of counter-propagating signals that has contributed to fundamental science and revolutionized advanced technology via a variety of significant devices including circulators and isolators (diodes) in electronics [1], optics [2-5], acoustics [6], and heat transfer [7]. While photonic metasurfaces have facilitated applications of free-space optics with an ultracompact lightweight advantage, such architecture can be potentially harnessed to achieve asymmetric free-space transport of light. Photonic gradient metasurfaces are two-dimensional ultrathin arrays of engineered meta-atoms (nanoscatterers) that mold optical wavefronts at subwavelength scale by imparting rapid phase changes along an interface [8-11]. These subwavelength-structured interfaces enable a custom-tailored electromagnetic response with unprecedented control over the fundamental properties of light, i.e., phase, amplitude, and polarization. Gradient metasurfaces aim to revolutionize optical designs by realizing virtually flat, ultrathin, and lightweight optics [10,11] that replaces bulky optical elements. Free-space wavefront molding at will by gradient metasurfaces encompasses, abnormal light bending [12,13], planar lenses [14,15], optical vortex generators [12,13], and photonic multitasking [16], etc. However, excluding time dependence and magnetic response, AT of light cannot be fundamentally achieved by any linear system [5] including linear metasurfaces.

Nonlinear processes or nonlinear materials can be employed to achieve AT [5]. Hence, the emerging nonlinear metasurfaces [17-19] may leverage AT. By combining nonlinear harmonic generation at interfaces and spatially varying effective nonlinear polarizability with controllable phase [17,18], nonlinear gradient metasurfaces (NGMs) offer nonlinear wavefront shaping [19,20]. The milestones of achieving extraordinary efficiency of nonlinear generation at a subwavelength thickness [21-24] and continuous control of the nonlinear phase [18,22] have opened a new paradigm of flat nonlinear optics. Previous demonstrations of AT aimed at on-chip (waveguide) architectures [1-4] or required propagation through inherently bulky configuration of a superlattice coupled to a nonlinear medium [6]. However, the highly desirable asymmetric free-space transport of light at optically thin flatland, in both transmission and reflection, has not yet been demonstrated. Here, we report the experimental observation of asymmetric free-space

transport of light at NGMs upon transmission and reflection. We also derived the generalized laws of refraction and reflection for NGMs, which were experimentally verified by angle-resolved anomalous refraction and reflection of the nonlinear light. Asymmetric free-space transport with metasurfaces provides a route to ultrathin lightweight optical platforms with unidirectional operation including ultrathin optical valves and diodes.

We consider a NGM as an optical interface between two media with an inherent rapid phase shift, wherein a nonlinear harmonic is generated (Fig. 1). The harmonic generation in NGMs requires revisiting the generalized Snell's laws of refraction and reflection originally introduced for linear gradient metasurfaces [13]. We consider an incident plane wave at an angle  $\theta_i$  at the fundamental harmonic (FH) and two light rays which are infinitesimally close to the actual light path (Fig. 1). In its general form known as the principle of stationary phase [25], Fermat's principle states that the variation of the phase accumulated along the actual light path is zero with respect to infinitesimal variations of the path. Accordingly, Fermat's principle corresponding to refraction at NGMs is formulated as

$$\left[ \frac{\omega_1}{c} n_i(\omega_1) \sin\theta_i dx - \frac{\omega_2}{c} n_t(\omega_2) \sin\theta_t dx \right] + (\omega_2 - \omega_1) \Delta t + d\phi = 0 \quad (1)$$

Here,  $\omega_1$  is the fundamental frequency, whereas  $\omega_2 = n\omega_1$  is the frequency of the generated nonlinear harmonic of order  $n$ ;  $c$  is the speed of light in vacuum,  $n_i(\omega_1)$  and  $n_t(\omega_2)$  are the refractive indices of the two media at the fundamental and nonlinear harmonic generation frequencies, respectively;  $\theta_t$  is the angle of refraction,  $dx$  is the infinitesimal distance between the locations in which the two light rays cross the interface, and  $d\phi$  is the phase difference between these two locations associated with the metasurface. While the first term is the optical path differences [Fig. 1(a)], the second expression is attributed to the time-harmonic dependence of electromagnetic fields. As the two light rays meet the interface at a time delay of  $\Delta t = \sin\theta_i dx / [c/n_i(\omega_1)]$ , the nonlinear harmonic is locally generated at different times along the NGM, giving rise to a temporal phase delay of  $(\omega_2 - \omega_1) \Delta t$  [see Fig. 1(a) inset]. Note that in stark contrast to linear gradient metasurfaces (i.e.,  $\omega_2 = \omega_1$ ), this term solely emerges in NGMs. By considering a constant phase gradient, we obtained the generalized Snell's law of refraction for NGMs

$$n_t(\lambda_2) \sin\theta_t - n_i(\lambda_1) \sin\theta_i = \frac{\lambda_1}{2\pi n} \frac{d\phi}{dx} \quad (2)$$

where  $\lambda_1 = 2\pi c/\omega_1$  and  $\lambda_2 = \lambda_1/n$  are the free-space wavelengths associated with the FH and the nonlinear harmonic generation, respectively.

Similarly, the generalized law of reflection corresponding to NGMs is

$$n_i(\lambda_2)\sin\theta_r - n_i(\lambda_1)\sin\theta_i = \frac{\lambda_1}{2\pi n} \frac{d\phi}{dx} \quad (3)$$

where  $\theta_r$  is the angle of reflection [Fig. 1(b)]. By introducing the anomalous refraction and reflection of the beams associated with the FH and nonlinear harmonic generation, these generalized laws of refraction and reflection govern the molding of optical wavefronts via custom-designed structured interfaces that mimic phase gradients. Note that this concept is unified, as for the fundamental wave (i.e.,  $n = 1$ ), the derived laws coincide with the generalized Snell's laws referring to linear gradient metasurfaces [13]. Beyond the scope of metasurfaces, these nonlinear generalized Snell's laws play a role of a working tool in nonlinear optics. Efficient generation of nonlinear light in bulky nonlinear materials is obtained by fulfilling the phase-matching condition [26], which is an arduous task requiring a compensation method for the inherent phase mismatch between the interacting waves propagating in the nonlinear media. The ultrathin thickness of NGMs imposes a reduced form of surface phase matching [Eq. (1)] which is naturally satisfied via the redirection of the generated nonlinear light (i.e., the angle of refraction or reflection).

We demonstrated experimentally the generalized laws of refraction and reflection in nonlinear structured interfaces via a plasmonic antenna array of gold nanorods coated with a thin nonlinear active layer of poly(9,9-dioctylfluorene) (PFO). The combination of high field enhancement from the resonant plasmonic structures and large third-order nonlinearity of the PFO gives rise to strong third harmonic generation (THG) in the formed gold-PFO hybrid nonlinear metasurface [18,27]. We imprinted rapid phase change in the nonlinear interface via the emerging concept of nonlinear geometric phase [18,22]. The spin-rotation coupling of light in NGMs induces nonlinear geometric phase of  $\phi(x,y) = (n \mp 1)\sigma\theta(x,y)$  for modes maintaining ( $\sigma, \sigma$  modes) or flipping ( $\sigma, -\sigma$  modes) the polarization of the incident fundamental wave, respectively [18]; here,  $\sigma = \pm 1$  is the polarization helicity (i.e., spin angular momentum of light in  $\hbar$  units, where  $\hbar$  is the reduced Planck's constant [28]) of the incident light corresponding to right and left circularly polarized light, respectively, and  $\theta(x,y)$  is the space-variant orientation angle of the anisotropic optical nanoantennas. NGMs based on the geometric phase, also referred as nonlinear Pancharatnam-Berry phase optical elements (see Supplemental

Material [29], Sec. 7), enable nonlinear wavefront shaping via spatially varying effective nonlinear polarizability with continuously controllable phase [18]. We realized a NGM with a constant phase gradient by locally rotating the nanorod antennas in such a way that their orientation angles vary linearly along the  $x$  direction [Fig. 2(a)]. Note that the FH modes resemble the response of linear metasurfaces, wherein the degenerated  $\sigma,\sigma$  modes exhibit ordinary refraction and reflection, whereas  $\sigma,-\sigma$  modes exhibit linear anomalous refraction and reflection [Fig. 2(b)]. In stark contrast to the FH, all THG ( $n = 3$ ) modes undergo nonlinear anomalous refraction and reflection, where  $\sigma,-\sigma$  modes experience stronger phase gradient than  $\sigma,\sigma$  modes [Fig. 2(b)]. Moreover, according to selection rules for harmonic generation [18], all polarization modes for both FH and THG signals are allowed with the two-fold rotational symmetry of the nanorod, enabling versatile linear and nonlinear wavefront shaping with the same structure.

We pumped the metasurface by a femtosecond laser at the wavelength of  $1.26 \mu\text{m}$  (i.e., the localized plasmon resonance of the hybrid metasurface; see Supplemental Material [29], Sec. 2) and imaged the  $k$ -space of the scattered light while varying the incident angle of the pump laser; by controlling the incident polarization, probing the desired polarization of the scattered light, and filtering out the wavelength of the pump laser via a bandpass filter, all FH and THG (at the wavelength of  $420 \text{ nm}$ ) modes were measured (see Supplemental Material [29], Sec. 4 for the experimental setup). The angles of refraction and reflection, extracted from the  $k$ -space imaging, as a function of the angle of incidence [Figs. 2(c) and 2(d), respectively] exhibit good agreement with theoretical calculations performed by the generalized laws of refraction and reflection for NGMs [Eqs. (2) and (3)]. Note that in transmission measurements, light incident from the substrate side is anomalously refracted to air by the metasurface interface [see Fig. 2(c) inset]; in reflection measurements, light incident from the substrate side is anomalously reflected to the substrate by the metasurface and then ordinarily refracted to air [see Fig. 2(d) inset]. In different ranges of angle of incidence, FH and THG modes reveal “negative” refraction and reflection [Figs. 2(c) and 2(d)]. The polarization-dependent critical angles for total internal reflection [Fig. 2(c)] and critical angles of incidence above which the reflected beam becomes evanescent [Fig. 2(d)] are evident for the FH and THG (see Supplemental Material [29], Sec. 3 for the detailed analysis).

By offering new functionalities that cannot be achieved with linear metasurfaces, NGMs take the molding of optical wavefronts to a new level. We specifically aimed at AT of light in ultrathin structured interfaces. Note that asymmetric transport was theoretically proposed in time-varying metasurfaces [30,31], i.e., interfaces wherein a temporal gradient is added to the conventional spatial gradient, which have not yet been realized. In the context of metasurfaces, for a given angle of incidence, we consider the angle of refraction in two consecutive scenarios that are linked by reversed propagation (RP); i.e., the angle of incidence in the bottom-to-top excitation scheme (light incident onto the metasurface from free space) is equal to the angle of refraction in the original top-to-bottom excitation (light incident onto the metasurface from the substrate) [see Fig. 3(a)]. The transport is referred as symmetric when the trajectory of light is reciprocal, i.e., the angle of refraction in the bottom-to-top excitation  $\theta_{t_2}$  is equal to the angle of incidence in the primary top-to-bottom excitation  $\theta_{i_1}$  [see Fig. 3(a)]. Otherwise (i.e.,  $\theta_{t_2} \neq \theta_{i_1}$ ), the transport is asymmetric. As the test for AT requires built-in polarization filters, the handedness of the circularly polarized beam launched from bottom to top is identical to the handedness of the circular polarization of the refracted beam in the top-to-bottom excitation; in a similar fashion, the polarization of the refracted beam in the top-to-bottom excitation is identical to the original polarization launched from top to bottom [see Fig. 3(a)]. This polarization requirement originates from the conservation of the helicity under time reversal, while reversing the direction of propagation. Similarly, the concept of AT in metasurfaces is introduced in reflection [Fig. 3(b)].

By measuring the angle-resolved refraction and reflection angles at both top-to-bottom [Figs. 2(c) and 2(d), respectively] and bottom-to-top (Supplemental Material [29], Fig. S6) excitation schemes and mapping the corresponding polarization modes, we characterized the transport of light in metasurfaces. We revealed that NGMs exhibit AT upon refraction and reflection for the  $\sigma, \sigma$  modes, while the  $\sigma, -\sigma$  modes exhibit symmetric transport [Figs. 3(c) and 3(d)]. In stark contrast, linear gradient metasurfaces show symmetric transport regardless of the polarization of the modes [Figs. 3(c) and 3(d) insets]. These observations are in good agreement with calculations based on the aforementioned generalized laws of refraction and reflection for NGMs. All-angle AT of free-space optical beams is a peculiar property of NGMs arising from the nonzero phase gradient imparted to the modes of the generated nonlinear harmonic that maintain the polarization state. The concept of AT in NGMs applies to any harmonic order; yet,



we chose to demonstrate THG to avoid arduous tasks in experiments as the degree of asymmetry increases with the generated harmonic order (see Supplemental Material [29], Sec. 6). Note that at both top-to-bottom and bottom-to-top excitations the incident wavelength is the fundamental wavelength; yet, the observed AT at NGMs is not optical isolation [5] as the nonlinear metasurface enables the conversion from the FH to the generated harmonic but not vice versa.

In summary, asymmetric free-space transport of light at an optically thin flatland is reported. Note that nonlinear anomalous refraction [17,18,20] or reflection [22-24] was previously observed only at normal incidence, wherein the spatial-temporal nonlinear phase delay vanishes; therefore, we probed its contribution to the nonlinear generalized Snell's laws by angle-dependent measurements. Moreover, the nonlinear generalized Snell's laws were derived as a working tool to explore the new functionality of asymmetric transport at NGMs. The generalized laws of refraction and reflection at nonlinear interfaces apply to the entire optical spectrum for suitable designer interfaces and may introduce new degrees of freedom in nonlinear optics for designing perfect phase matching. This study may also inspire the merging of metasurface principles and nonreciprocity, where one-way invisibility cloak, ultrathin optical diodes and arbitrary nonreciprocal beam steering are envisioned.

## References

- [1] N. Bender, S. Factor, J. D. Bodyfelt, H. Ramezani, D. N. Christodoulides, F. M. Ellis, and T. Kottos, Observation of asymmetric transport in structures with active nonlinearities, *Phys. Rev. Lett.* **110**, 234101 (2013).
- [2] L. Fan, J. Wang, L. T. Varghese, H. Shen, B. Niu, Y. Xuan, A. M. Weiner, and M. Qi, An all-silicon passive optical diode, *Science* **335**, 447 (2012).
- [3] H. Lira, Z. Yu, S. Fan, and M. Lipson, Electrically driven nonreciprocity induced by interband photonic transition on a silicon chip, *Phys. Rev. Lett.* **109**, 033901 (2012).
- [4] L. Feng, Y.-L. Xu, W. S. Fegadolli, M.-H. Lu, J. E. B. Oliveira, V. R. Almeida, Y.-F. Chen, and A. Scherer, Experimental demonstration of a unidirectional reflectionless parity-time metamaterial at optical frequencies, *Nat. Mater.* **12**, 108 (2013).
- [5] D. Jalas, A. Petrov, M. Eich, W. Freude, S. Fan, Z. Yu, R. Baets, M. Popović, A. Melloni, J. D. Joannopoulos *et al.*, What is – and what is not – an optical isolator, *Nat. Photonics.* **7**, 579 (2013).
- [6] B. Liang, X. S. Guo, J. Tu, D. Zhang, and J. C. Cheng, An acoustic rectifier, *Nat. Mater.* **9**, 989 (2010).
- [7] C. W. Chang, D. Okawa, A. Majumdar, and A. Zettl, Solid-state thermal rectifier, *Science* **314**, 1121 (2006).
- [8] Z. Bomzon, V. Kleiner, and E. Hasman, Pancharatnam-Berry phase in space-variant polarization-state manipulations with subwavelength gratings, *Opt. Lett.* **26**, 1424 (2001).
- [9] Z. Bomzon, G. Biener, V. Kleiner, and E. Hasman, Space-variant Pancharatnam-Berry phase optical elements with computer-generated subwavelength gratings, *Opt. Lett.* **27**, 1141 (2002).
- [10] A. V. Kildishev, A. Boltasseva, and V. M. Shalaev, Planar photonics with metasurfaces, *Science* **339**, 1232009 (2013).
- [11] N. Yu and F. Capasso, Flat optics with designer metasurfaces, *Nat. Mater.* **13**, 139 (2014).
- [12] N. Shitrit, I. Bretner, Y. Gorodetski, V. Kleiner, and E. Hasman, Optical spin Hall effects in plasmonic chains, *Nano Lett.* **11**, 2038 (2011).
- [13] N. Yu, P. Genevet, M. A. Kats, F. Aieta, J.-P. Tetienne, F. Capasso, and Z. Gaburro, Light propagation with phase discontinuities: Generalized laws of reflection and refraction, *Science* **334**, 333 (2011).

- [14] E. Hasman, V. Kleiner, G. Biener, and A. Niv, Polarization dependent focusing lens by use of quantized Pancharatnam-Berry phase diffractive optics, *Appl. Phys. Lett.* **82**, 328 (2003).
- [15] M. Khorasaninejad, W. T. Chen, R. C. Devlin, J. Oh, A. Y. Zhu, and F. Capasso, Metalenses at visible wavelengths: Diffraction-limited focusing and subwavelength resolution imaging, *Science* **352**, 1190 (2016).
- [16] E. Maguid, I. Yulevich, D. Veksler, V. Kleiner, M. L. Brongersma, and E. Hasman, Photonic spin-controlled multifunctional shared-aperture antenna array, *Science* **352**, 1202 (2016).
- [17] N. Segal, S. Keren-Zur, N. Hendler, and T. Ellenbogen, Controlling light with metamaterial-based nonlinear photonic crystals, *Nat. Photonics* **9**, 180 (2015).
- [18] G. Li, S. Chen, N. Pholchai, B. Reineke, P. W. H. Wong, E. Y. B. Pun, K. W. Cheah, T. Zentgraf, and S. Zhang, Continuous control of the nonlinearity phase for harmonic generations, *Nat. Mater.* **14**, 607 (2015).
- [19] G. Li, S. Zhang, and T. Zentgraf, Nonlinear photonic metasurfaces, *Nat. Rev. Mater.* **2**, 17010 (2017).
- [20] S. Keren-Zur, O. Avayu, L. Michaeli, and T. Ellenbogen, Nonlinear Beam Shaping with Plasmonic Metasurfaces, *ACS Photonics* **3**, 117 (2016).
- [21] J. Lee, M. Tymchenko, C. Argyropoulos, P.-Y. Chen, F. Lu, F. Demmerle, G. Boehm, M.-C. Amann, A. Alù, and M. A. Belkin, Giant nonlinear response from plasmonic metasurfaces coupled to intersubband transitions, *Nature* **511**, 65 (2014).
- [22] M. Tymchenko, J. S. Gomez-Diaz, J. Lee, N. Nookala, M. A. Belkin, and A. Alù, Gradient nonlinear Pancharatnam-Berry metasurfaces, *Phys. Rev. Lett.* **115**, 207403 (2015).
- [23] J. Lee, N. Nookala, J. S. Gomez-Diaz, M. Tymchenko, F. Demmerle, G. Boehm, M.-C. Amann, A. Alù, and M. A. Belkin, Ultrathin second-harmonic metasurfaces with record-high nonlinear optical response, *Adv. Opt. Mater.* **4**, 664 (2016).
- [24] N. Nookala, J. Lee, M. Tymchenko, J. S. Gomez-Diaz, F. Demmerle, G. Boehm, K. Lai, G. Shvets, M.-C. Amann, A. Alu, and M. Belkin, Ultrathin gradient nonlinear metasurface with a giant nonlinear response, *Optica* **3**, 283 (2016).
- [25] E. Hecht, *Optics* (Addison Wesley, Boston, 1997).
- [26] R. W. Boyd, *Nonlinear Optics* (Academic Press, New York, 2008).

- [27] S. Chen, G. Li, F. Zeuner, W. H. Wong, E. Y. B. Pun, T. Zentgraf, K. W. Cheah, and S. Zhang, Symmetry-selective third-harmonic generation from plasmonic metacrystals, *Phys. Rev. Lett.* **113**, 033901 (2014).
- [28] K. Y. Bliokh, F. J. Rodríguez-Fortuño, F. Nori, and A. V. Zayats, Spin-orbit interactions of light, *Nat. Photonics* **9**, 796 (2015).
- [29] See Supplemental Material for the sample fabrication, characterization of the plasmonic resonance of nanorods and the third harmonic generation from the PFO, optical setup for angle-resolved  $k$ -space imaging of anomalous refraction and reflection from nonlinear gradient metasurfaces, anomalous nonlinear refraction at bottom-to-top excitation, derivation of the asymmetric transport of light at nonlinear gradient metasurfaces, and representation of nonlinear Pancharatnam-Berry phase optical elements.
- [30] Y. Hadad, D. L. Sounas, and A. Alu, Space-time gradient metasurfaces, *Phys. Rev. B* **92**, 100304 (2015).
- [31] A. Shaltout, A. Kildishev, and V. Shalaev, Time-varying metasurfaces and Lorentz nonreciprocity, *Opt. Mater. Express* **5**, 2459 (2015).

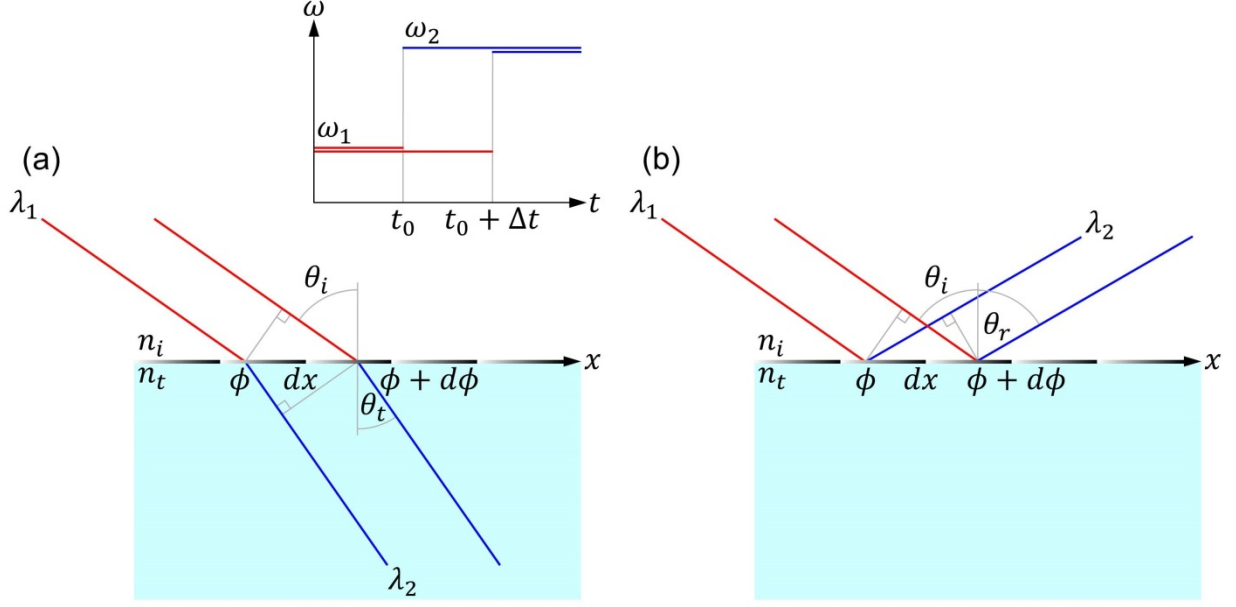


FIG. 1. Generalized laws of refraction and reflection at nonlinear gradient metasurfaces. (a),(b) Schematics used to derive the generalized laws of refraction and reflection for NGMs, respectively, wherein the optical path differences and the rapid phase shift (grayscale pattern) introduced by the metasurface are depicted. Red and blue rays correspond to rays of light at the fundamental wavelength  $\lambda_1$  and at the wavelength of the generated nonlinear harmonic  $\lambda_2$ , respectively.  $\phi$  and  $\phi + d\phi$  are the phase shifts at the two locations in which the rays cross the interface. The inset in (a) illustrates the temporal phase delay originating from the time difference  $\Delta t$  in the generation of the nonlinear harmonic between the two crossing locations. The three factors of optical path differences, spatial-temporal nonlinear phase delay, and metasurface-induced phase shift give rise to the nonlinear generalized Snell's laws of refraction  $n_t(\lambda_2)\sin\theta_t - n_i(\lambda_1)\sin\theta_i = \frac{\lambda_1}{2\pi n} \frac{d\phi}{dx}$  and reflection  $n_i(\lambda_2)\sin\theta_r - n_i(\lambda_1)\sin\theta_i = \frac{\lambda_1}{2\pi n} \frac{d\phi}{dx}$ , where  $n$  is the order of the generated nonlinear harmonic.

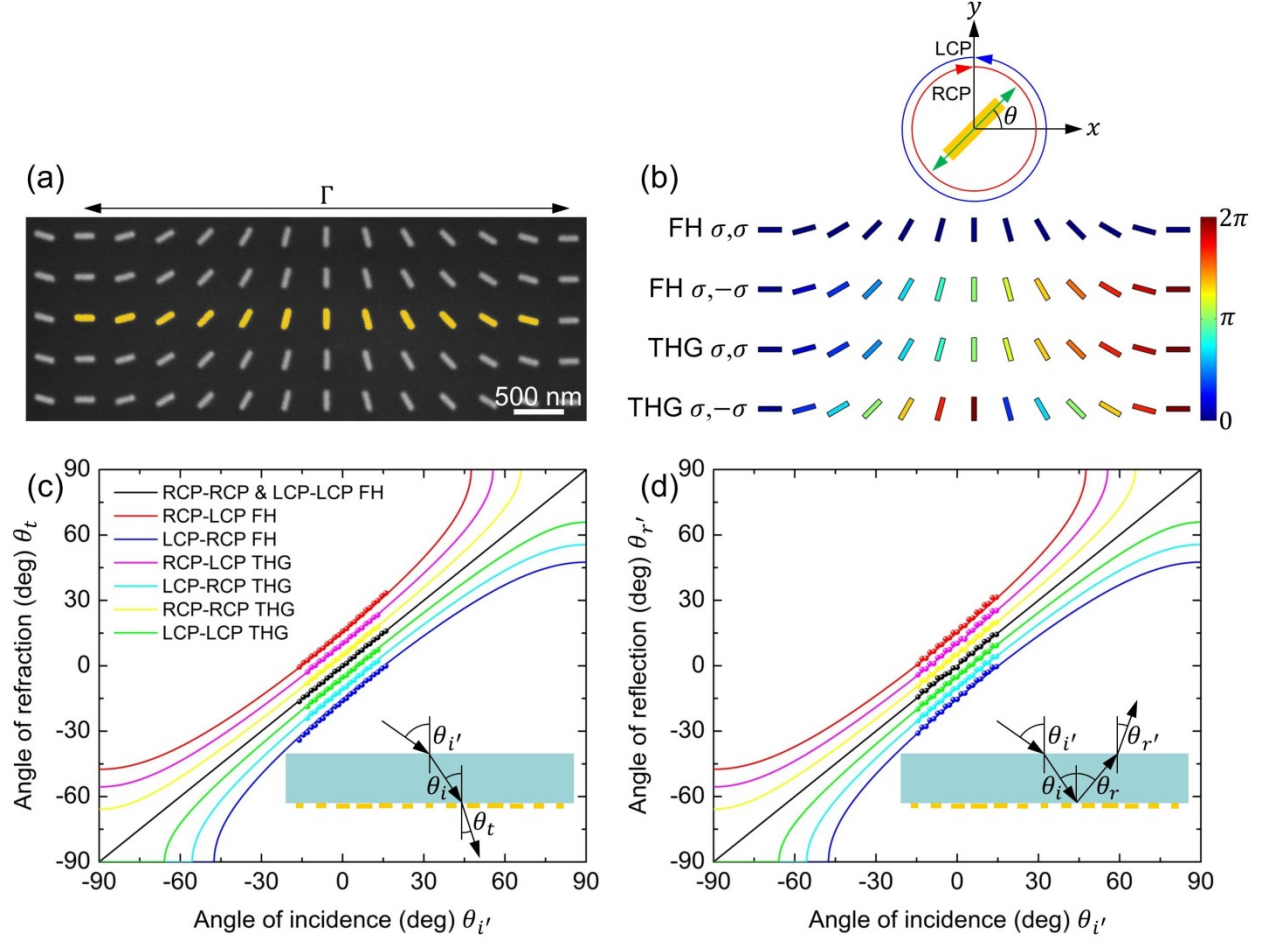


FIG. 2. Anomalous refraction and reflection from nonlinear gradient metasurfaces. (a) Scanning electron microscope image of the NGMs. The unit cell of the NGMs (yellow) comprises twelve gold nanorod antennas, where their orientation angles  $\theta(x,y)$  rotate linearly to generate a constant phase gradient. The width and length of each nanorod are 50 nm and 240 nm, respectively, and the thickness is 30 nm. The unit cell repeats with a periodicity  $\Gamma$  of 4.8  $\mu\text{m}$  along the  $x$  direction and 400 nm along the  $y$  direction. The gold metasurface was coated with a 100-nm-thick PFO layer to form metal-organic hybrid nonlinear metasurfaces. (b) Same metasurface structure introduces different phase distributions for the FH and THG (resembling linear and NGMs, respectively). Colors filling the nanorods depict the local phase. The FH beam experiences a constant phase for the modes maintaining the polarizations ( $\sigma, \sigma$  modes), while the modes flipping the polarizations ( $\sigma, -\sigma$  modes) experience a linear phase profile from 0 to  $2\pi$ . The THG beam experiences linear phase profiles from 0 to  $2\pi$  and from 0 to  $4\pi$  for  $\sigma, \sigma$  and  $\sigma, -\sigma$  modes, respectively. The phase profiles portrayed by color correspond to right circular polarization (RCP) excitation ( $\sigma = +1$ ); for left circular polarization (LCP) excitation ( $\sigma = -1$ ),

the trends of the phase profiles are similar but with the opposite slope. (c),(d) Angles of refraction ( $\theta_t$ ) and reflection ( $\theta_{r'}$ ) versus the angle of incidence ( $\theta_{i'}$ ), respectively. Modes are labelled with the incident-analyzed polarization state. Lines correspond to theoretical calculations performed by the generalized laws of refraction and reflection for NGMs [Eqs. (2) and (3)], whereas dots refer to measured data. Error bars (not shown) are smaller than the size of the data points. All angles were measured in free space as shown in the insets.

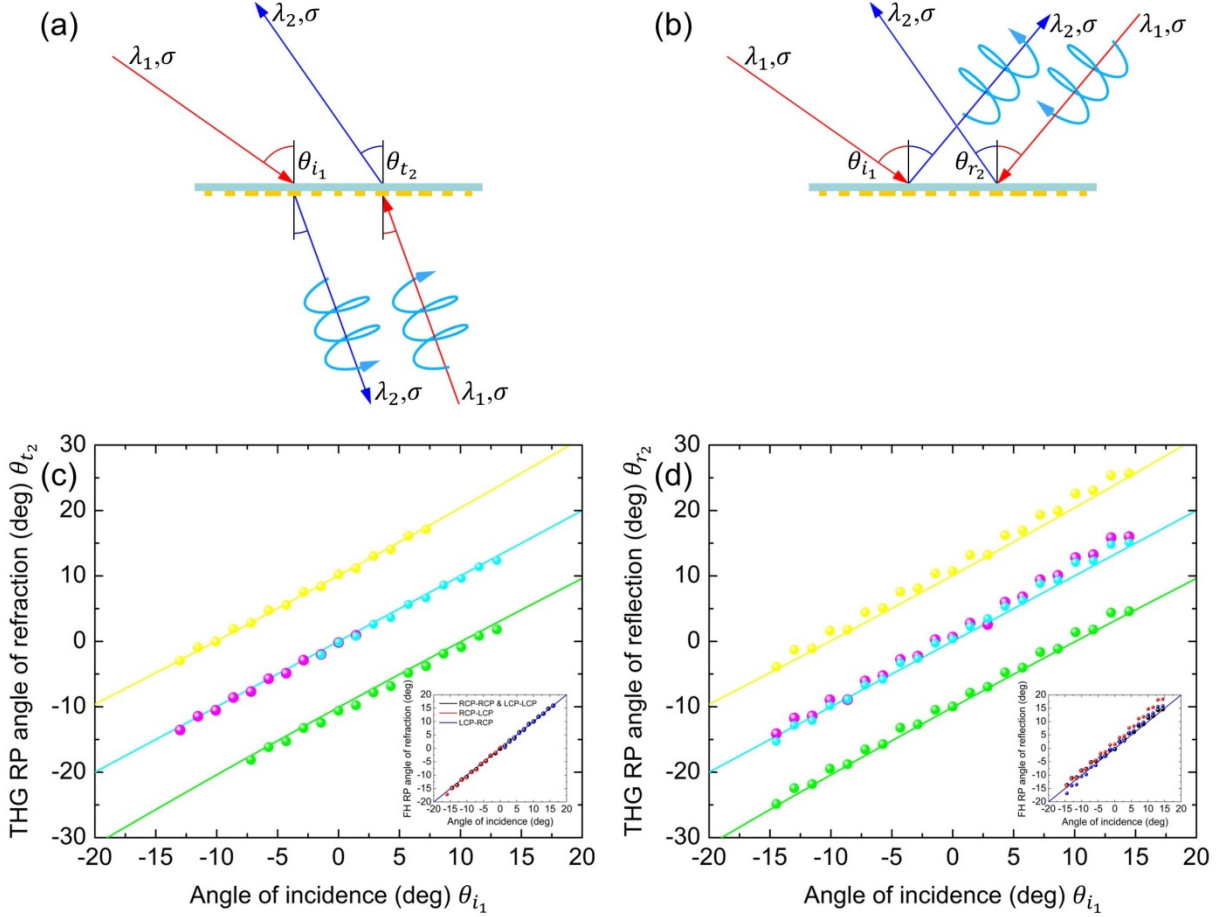


FIG. 3. Asymmetric transport at nonlinear gradient metasurfaces. (a),(b) Schematics of the concept of AT at NGMs for refraction and reflection, respectively. We first consider the angle of refraction or reflection for a given angle of incidence  $\theta_{i_1}$ ; then, we excite the metasurface from the opposite side, where the angle of incidence is set to the obtained angle of refraction or reflection in the original excitation (i.e., RP path). Moreover, the handedness of the circular polarization of these two beams is identical owing to RP. The transport of light is asymmetric when the angle of refraction  $\theta_{t_2}$  or reflection  $\theta_{r_2}$  in the excitation from the opposite side is different from  $\theta_{i_1}$ . (c),(d) THG RP angles of refraction ( $\theta_{t_2}$ ) and reflection ( $\theta_{r_2}$ ) versus the angle of incidence in the original excitation ( $\theta_{i_1}$ ), respectively. Lines correspond to calculations based on the generalized laws of refraction and reflection at NGMs, whereas dots refer to measured data. All angles were measured in free space. The polarization state of the modes refers to the original excitation. The insets in (c) and (d) are the corresponding results for the FH (linear metasurfaces).